

## Computational scheme for the prediction of metal ion binding by a soil fulvic acid

J.A. Marinsky<sup>a</sup>, M.M. Reddy<sup>b</sup>, J.H. Ephraim<sup>c,\*</sup>, A.S. Mathuthu<sup>d</sup>

<sup>a</sup> Department of Chemistry, State University of New York at Buffalo, Buffalo, NY 14214, USA

<sup>b</sup> US Geological Survey, Denver Federal Center, Lakewood, CO 80225, USA

<sup>c</sup> Linköping University, Department of Water and Environmental Studies, S-58183 Linköping, Sweden

<sup>d</sup> Department of Chemistry, University of Zimbabwe, P.O. Box MP 167, Mount Pleasant, Harare, Zimbabwe

Received 4 July 1994; accepted 2 October 1994

### Abstract

The dissociation and metal ion binding properties of a soil fulvic acid have been characterized. Information thus gained was used to compensate for salt and site heterogeneity effects in metal ion complexation by the fulvic acid. An earlier computational scheme has been modified by incorporating an additional step which improves the accuracy of metal ion speciation estimates. An algorithm is employed for the prediction of metal ion binding by organic acid constituents of natural waters (once the organic acid is characterized in terms of functional group identity and abundance). The approach discussed here, currently used with a spreadsheet program on a personal computer, is conceptually envisaged to be compatible with computer programs available for ion binding by inorganic ligands in natural waters.

**Keywords:** Fulvic acids; Computational scheme; Metal ion binding prediction

### 1. Introduction

The solution chemistry of natural organic acids is not fully understood even though considerable advances have been made over the past decade. This short-coming is a consequence of a combination of factors, including the following: the absence of a unique structure of humic substances, the variation in the methods of isolation and extraction and the absence of specific analytical methods suitable only for humic substances. The absence of a total understand-

ing has thus necessitated the need to model. The first problem with modelling lies with the manner in which these natural organic acids are conceptualised. A perusal through the literature reveal the following as examples of how natural organic acids (humic and fulvic acids) are conceptualised.

(1) Strongly associated aggregates of acids, each of comparatively low molecular weight [1].

(2) An assemblage of identical mean fulvic acid units; a fulvic acid unit is a hypothetical macromolecule that contains one or more distinct classes of acidic functional groups [2].

(3) An oligoelectrolyte (intermediate between simple ions and true polyelectrolytes) composed of impenetrable charged spheres [3].

\* Corresponding author.

(4) An assemblage of relatively small amphiphilic moieties which are slightly different but composed of four to five predominant separate acidic sites with each site characterised by a distribution of average acidic strength. [4].

These conceptualisations have led to the development of two major types of modelling, namely the discrete ligand approach and the continuous distribution approach. In the discrete ligand approach, the observed behaviour has been attributed to a limited number of predominant sites. Ion binding by humic substances which is described in terms of complexation at discrete sites is postulated to be modified by electrostatic attraction and/or repulsion and non-specific binding due to counterion accumulation [5]. In the model, variations in apparent binding strengths in terms of a collection of abundant major proton-dissociating groups (COOH, phenolic-OH) are combined with electrostatic effects. Eight proton-dissociating sites are envisaged and the metal binding is postulated to occur either at single proton-dissociating site (monodentate) or in a bidentate fashion. There are seven adjustable parameters for fitting proton dissociation and an additional two parameters for each additional cation that can bind at the acid-dissociating sites [5].

In the recent oligoelectrolyte model [3], humic substances are again represented as impenetrable spheres and the electrostatic effect is calculated using approximations of the nonlinear Poisson-Boltzmann equation. The "local" concentration of metal ion near the charged polyions,  $[M^{z+}]_{loc}$ , is related to the concentration of the metal ion in the bulk solution,  $[M^{z+}]_{sol}$  as follows:

$$[M^{z+}]_{loc} = \lambda^z [M^{z+}]_{sol} \quad (1)$$

where  $\lambda$ , the electrostatic factor which is also interpreted as a ratio of polyion activities when the molecular spheres envisaged are penetrable, i.e., allow diffusible components into its domain. The model consists of a total of 14 parameters which may be reduced to 9.

In the continuous distribution model, the properties of the various sites are assumed to overlap thus warranting the use of statistical methods for their estimation. The basis of the affinity distribution model is the representation of the complexation parameters by a probability density function [6–8].

Binding of ions to humic substances is considered to be influenced by a variable electrical potential and by a variety of binding sites [8]. Humic substances are treated as an ensemble of identical heterogeneous polyelectrolytes for which an average potential holds near all groups. The proton concentration at the location of the binding sites, is also related to the bulk proton concentration by using the Poisson-Boltzmann equation. Such electrostatic corrections are employed to obtain a "master curve" from which intrinsic proton affinity distribution may be determined.

However, in the application of the continuous distribution model to the acid-base properties of natural organic acids (humic and fulvic acid), the overall acidity is factored into two where a lower  $pK_a$  value, normally around 4.2 represents the carboxylic distribution, while a higher  $pK_a$  value, normally around 9.1 represents the phenolic distribution. This division yields an equivalent result as in the discrete approach by considering two major acidic sites.

Another example of the continuous distribution model is the normal distribution model [9,10] where the distribution of ligands in the molecule is described by a mean ( $\mu$ ) and a variance ( $\sigma^2$ ) as follows:

$$\frac{C_i}{C_L} = \frac{1}{\sigma\sqrt{2\pi}} \exp\left[-\frac{1}{2}\left(\frac{\mu - pK_i}{\sigma}\right)^2\right] dpK \quad (2)$$

where  $C_i/C_L$  is the mole fraction of the ligand in the interval  $dpK$ ,  $pK_i$  is the negative logarithm of the dissociation constant for the proton binding,  $\sigma$  is the standard deviation and  $\mu$  is the mean  $pK$  of the proton binding to the humic substance [9,10]. Incorporating the above expression into that for the fraction of metal bound (in metal-humate systems) and again assuming a continuous distribution yields the expression:

$$\theta_{cal} = \frac{1}{\sigma\sqrt{2\pi}} \int \frac{[M]10^\kappa}{1 + [M]10^\kappa} \times \exp\left[-\frac{1}{2}\left(\frac{\mu - pK_i}{\sigma}\right)^2\right] dpK \quad (3)$$

Application of the Gaussian distribution model to humic substances readily distinguishes a two-ligand

mixture from a continuous distribution of ligands and can also distinguish between unimodal and bimodal distributions [9].

In the differential equilibrium function model [11–13], a continuous distribution of sites is assumed where the macroscopic binding functions,  $K_{\text{macro}}$ , is interpreted in terms of the microscopic binding constants,  $K_{\text{micro}}$ , as follows:

$$K_{\text{macro}} = \frac{M_b}{M_f L_T^f} = \frac{\sum K_{\text{micro}} [L_i^f]}{[L_T^f]} \quad (4)$$

In the above equation,  $M_b$  is the total bound metal,  $M_f$  is the free metal,  $L_T^f$  represents all sites not combined with M while  $L_i^f$  represents the concentrations of the microscopic sites not combined with the metal [11–13]. Since the binding sites are assumed to overlap, the summation in the above equation is replaced with an integral as follows:

$$K_{\text{macro}} L_T^f = \int KL^f(K, M) dk = \int K \frac{L(K)}{(1 + KM)} dk \quad (5)$$

where  $L^f(K, M)$  is considered to be a continuous function of  $K$  and the amount of metal,  $M$ , present.

The choice of which model to employ in the description of metal–humate interactions depends on the objective of the data analysis. The discrete multi-ligand approach is easily adapted to experimental data using graphical methods [14] and as such amenable to the prediction of metal–humate interactions by easy incorporation into existing chemical speciation computer programs, e.g., MINEQL [15]. The disadvantages of the discrete ligand model include the fact that the identified ligands may not be representative of the actual binding sites in the humic substance, the difficulty in its adaptation outside the range of calibration and the tendency to underestimate metal humate interactions at very low metal ion concentration [16].

Whereas the continuous distribution model probably approaches the complexity of natural organic acids, its short-coming is its adaptation into anticipating the sequestering of metal ions. It has, therefore, been argued that the continuous distribution model serves primarily as a first step towards identifying

the most probable distribution of the acidic functionalities in the natural organic acids [16]. In effect, the application of the affinity distribution model [8] is intrinsically similar to the discrete model as employed to humic substances [3,17].

New advances in the description of proton and metal ion binding by humic substances have been motivated by the adaptation of an approach originally designed for synthetic polelectrolytes to humic substances [18–20]. It has to be noted that in most of the models described above, the need to separate electrostatic effects from functional group heterogeneity in metal–humate interactions was not realised until after the development of the unified physicochemical approach [21]. The intrinsic difference between the unified physicochemical approach and the other models is that in the unified physicochemical approach considerable emphasis is placed on understanding the chemistry of the ligand in terms of the probable functional groups while in the other methods, the ligand is most of the time considered as a “black box” with emphasis placed on solving mathematical equations in curve-fitting exercises.

The objectives of this paper may be summarised as follows:

- (a) to review the original site-binding model and its first application;
- (b) to identify shortcomings in the approach and propose correlations;
- (c) to show that the incorporation of an additional step to the earlier algorithm improves the metal ion speciation.

## 2. A review of the site-binding model and its first application

### 2.1. Formulation of model

Earlier studies of the Armadale Horizons Bh fulvic acid [22] show that 24.5% of the total acidity measurable in aqueous solution is attributable to a fairly strong carboxylic acid component characterized by an intrinsic  $pK_a$  of 1.8 (site I), 30.4% is attributable to a somewhat weaker carboxylic acid

with an intrinsic  $pK_a$  of 3.4 (site II), and 22.4% to a still weaker carboxylic acid characterized by an intrinsic  $pK_a$  of 4.2 (site III). The remaining 22.7% of the acid measurable in aqueous media was assigned to an acidic alcohol (enol) with an intrinsic  $pK_a$  of 5.7 (site IV).

Also deduced from these earlier characterization studies was the observation that two of these four acid sites had to contain two additional acid groups too weak to be detected by standard titration procedures. This hypothesis explained extra release of protons in the presence of excess Eu(III) or Cu(II) ion. A two-fold greater release of extra proton in the presence of the Cu(II) ion than in the presence of the Eu(III) ion influenced assignment of the carboxylic acid associated with site II ( $pK_a = 3.4$ ) to one of the two very weakly acid phenolic OH groups presumed to be involved in the bidentate configurations needed for the extra proton release. The second bidentate combination was identified with the weak acid alcohol (site IV) and the other phenolic OH group *ortho* to it [22].

The initial exclusive assignment of phenolic OH groups to the two bidentate sites identified had to be modified to accommodate the pattern of Cu(II), Co(II), Zn(II) and Eu(III) interaction with the Armadale Horizons Bh fulvic acid [23–26]. The highly selective binding of low concentration levels of Cu(II) ion at low pH levels was best accounted for by substituting an amine group for 23.3% of the OH groups initially assigned to the site II carboxylic acid [23]. Replacement of the salicylic acid-like functionality with a  $\beta$ -carboxymethylaminopropionic acid-like moiety led to binding consistent with experimental observation [23].

Replacement of 10% of the very weakly acidic phenolic OH of the dihydroxyl moiety postulated with a carbonyl group corrected for the severe underestimate of binding when the dihydroxyl chelation path was considered to be the only one available [26]. The more easily accessible path to chelation provided by the carbonyl group removed the earlier tendency to underestimate binding patterns severely as pH levels increased.

With this picture of the fulvic acid molecule metal ion binding could be accounted for in the following way. Eight metal ion-bound species, four unidentate at site I, II, III and IV and four chelated at site II and

IV were presumed to form by simultaneous interaction of the metal ion with the weak acid groups of fulvic acid. The quantity of metal ion bound at each site depends on site abundance and the ion association constant. Literature values of the metal ion constants of complex species most closely resembling those expected to be formed [27] were used whenever possible to anticipate the various reaction paths [23–26].

## 2.2. Development of computational scheme

The above site-binding model was used to develop the first computational scheme for estimating copper binding to a soil fulvic acid. The measured pH and pCu values were used in the model to estimate the total quantity of copper-bound species,  $\Sigma Cu_{b,expt}$ , at each experimental pH value. To monitor the predictive quality of the computational scheme at different salt concentration levels the model-based estimates of  $Cu^{2+}$  ion bound species,  $\Sigma Cu_{b,calc}$ , were compared with the experimentally-based values,  $\Sigma Cu_{b,expt}$ . The  $\Sigma Cu_{b,expt}$  parameter was obtained through measurement of free  $Cu^{2+}$  ion during the stepwise titration with standard base of the  $Cu^{2+}$  ion containing soil fulvic acid, simple salt systems prepared for study [23].

Uncertainties introduced in the initial program are noted and discussed in the course of this review. Remedial steps taken to remove them are then examined in some detail. They provide the basis for the refined computational scheme eventually presented.

### The initial computational scheme

To initiate examination of the equilibria encountered in Cu(II) ion, fulvic acid, simple salt systems estimates of fulvic acid group dissociation at each experimental pH prior to complexation of the Cu(II) ion were sought first. The overall degree of dissociation of the fulvic acid,  $\alpha_o$ , was obtained from the experimental pH by interpolating  $pK_a$  values from a plot of  $pK_a$  versus pH for the Cu(II) ion free but otherwise equivalent fulvic acid system [24]. The value of  $\alpha_o$  was then resolvable either from a plot of  $pK_a$  versus  $\alpha_o$  [24] in the Cu(II) ion free system at

the salt concentration level of the system under investigation or simply from use of Eq. 6.

$$\text{pH} - \text{p}K_a = \log\left(\frac{\alpha_o}{1 - \alpha_o}\right) \quad (6)$$

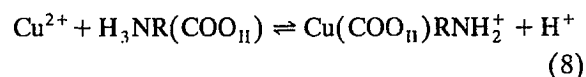
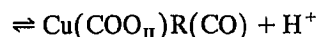
The appropriate correction for concentration enhancement of the  $\text{H}^+$  ion in the counterion concentrating region of the fulvic acid molecule was then estimated using the term  $(\text{p}K_I - \text{p}K_{I \geq 1.0 M})$ , denoted as  $\Delta\text{p}K$ , versus  $\alpha_o$  curves [22]. The fractional dissociation,  $\alpha_n$ , of the three carboxylic acids and the one enol was calculated with Eq. 7.

$$\text{p}K_{a, \text{intr}, n} + \Delta\text{p}K = \text{pH} - \log\left(\frac{\alpha_n}{1 - \alpha_n}\right) \quad (7)$$

In this equation the subscript  $n$  identifies weak acid sites ( $n = \text{I, II, III and IV}$ ),  $\text{p}K_{a, \text{intr}, n}$  corresponds to the intrinsic  $\text{p}K_a$  assigned earlier to the weak acid associated with that particular site,  $\Delta\text{p}K$  is as defined earlier, and  $\alpha_n$  is the fractional dissociation of the  $n$ th site. The quantity of each complexed species was calculated from  $\alpha_n$  in a sequence of computations [23]. These computations used literature-based values [27] for formation constants of the eight Cu(II) ion bound species expected to be formed. The linear relation between the published log of the complexation constant,  $\log(\beta_{\text{Cu-RCOOH}})$ , values of unidentate Cu(II) complexes of monocarboxylic acids and their corresponding acid dissociation constant [28] was employed to assign stability constant values to the unidentate Cu(II) species formed with the four acid (COOH and OH) sites of the Armadale fulvic acid. These stability constants,  $\beta_1 = 2.5 \times 10^1$ ,  $\beta_2 = 5.0 \times 10^1$ ,  $\beta_3 = 1.7 \times 10^2$  and  $\beta_4 = 2.62 \times 10^2$ , were used in the mass action expressions to calculate the formation of unidentate complexes to the respective acid sites,  $\text{CuA}_n^+$ , as a function of  $\alpha_n$  and pH.

Equations that described the curves employed to facilitate resolution of the  $\alpha_o$  and Donnan potential terms, ( $\Delta\text{p}K$ ), graphically were substituted to reach this objective with an algorithm used with a personal computer. One (site II) of the two bidentate sites (site II and site IV) provided two complexation reactions with the Cu(II) ion. 23% of the phenolic OH groups *ortho* to this carboxylic acid group (site II) were replaced by an amine group to define the second site II–Cu ion reaction when it was found

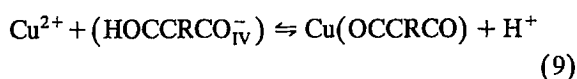
that this led to better agreement between calculation and experiment. Chelates thus formed were considered analogous to complexes formed with salicylic acid (first reaction in Eq. 8) and methyl amino propionic acid (second reaction in Eq. 8).



Computations of chelate formation as a function of  $\alpha$  and pH used literature-based formation constant values [27] for the mass action expressions for the reactions in Eq. 8. These parameters, multiplied by the corresponding dissociation constants of the dibasic acids involved in the chelation reactions, define the equilibrium constants for the reactions shown (Eq. 8), to facilitate estimate of copper chelated complex formation. Because the concentration of free bidentate ligand is not accessible, the mass action expression for the complexation reaction could not be used for this purpose. The  $\beta$  value of  $4.7 \times 10^{10}$  reported for the copper salicylate chelate at an ionic strength of 0.1 [27], estimated to reach a value of  $2.7 \times 10^{11}$  at infinite dilution, was combined with the approximate  $K_a$  value of  $10^{-13}$  assignable to the dissociation of the phenolic OH group of salicylic acid [27] to resolve a value of 0.027 for  $K_{\text{exch}, 1}$ , the equilibrium constant of the first reaction in Eq. 8 above. The value of 16 assigned to  $K_{\text{exch}, 2}$ , the equilibrium constant for the second reaction in Eq. 8, is somewhat larger than the value of 10 obtained with methyl aminopropionic acid [27], the molecule selected to model the change in metal ion binding properties associated with the site II carboxylic acid when the amine group is substituted for the phenolic OH. In this instance both the formation constant of the chelate,  $\beta_{\text{CuChel}} = 2.8 \times 10^{10}$  [27], and the dissociation constant of the second ionization step in the dibasic acid,  $K_2 = 3.5 \times 10^{-10}$  [27], were measured at an ionic strength of 0.1. Corrections for non-ideality of the  $\text{Cu}^{2+}$  and  $\text{H}^+$  ions at this ionic strength increase the product of  $\beta_{\text{CuChel}}$  and  $K_2$  from 9.8 to the value of 16 used in our computations. Simultaneous binding of Cu(II) to one or both of the coordinating groups associated with site IV (OH) were con-

ducted in a similar manner. Complexation reactions include the weakly acidic alcohol assigned to site IV and one of two bidentate reactions of either the phenolic OH group *ortho* to it or a carbonyl group substituted for the phenolic OH 10% of the time. A value of  $10^9$  was assigned to the formation constant of the dihydroxyl chelate of Cu(II) ion that was presumed to be nine times more prevalent than the keto, enol chelate of Cu(II).

Inaccessibility of the concentration of the fully dissociated dihydroxyl functionality associated with site IV once again necessitated the circuitous route first described to facilitate computation of the extent of  $\text{Cu}^{2+}$  ion chelation by this moiety. For this purpose, use was made of a displacement reaction, as before



A value of  $2 \times 10^{-2}$  was assigned to  $K_{\text{exch}3}$ , the equilibrium constant for this reaction, in order to provide the path to assess  $\text{Cu}^{2+}$  ion binding by 90% of the site IV chelation capacity. To reach this parameter a  $K_a$  value of  $2 \times 10^{-11}$  was combined with the  $10^9$  value chosen for the formation constant of the copper chelated complex. The assignment of a value of  $10^9$  to the formation constant of the dihydroxyl chelate of Cu(II) is consistent with published values of oxygen-linked bidentate complexes of  $\text{Cu}^{2+}$  [27] and was assigned to the formation constant of the keto, enol chelate of copper as well. A formation constant of  $10^6$  for the  $\text{Co}^{2+}$  and  $\text{Zn}^{2+}$  bidentate complexes formed with the postulated hydroxyl, carbonyl group in the tracer-level studies [24,26] supports this assignment. When multiplied by a factor of  $10^3$  to account for the extra stability of the Cu chelate, given by the ratio of the formation constants of the related acetyl acetate molecule [27], this value of  $10^9$  is obtained.

Mass action-based expressions were corrected for Debye-Hückel long-range interactions by employing the single ion activity coefficient for  $\text{Cu}^{2+}$ -ion,  $\gamma_{\text{Cu}}$ , from Kielland [29].

Donnan potential corrections for  $\text{H}^+$  ion, ( $\Delta pK$ ), used in the evaluation of  $\alpha_o$ , was presumed to also apply to the  $\text{Cu}^{2+}$  ion. This term is squared when used for the divalent  $\text{Cu}^{2+}$  ion. Removal of free

$\text{Cu}^{2+}$  ion from solution by hydrolysis was considered when the pH of the system reaches and exceeds a value of 6. This correction was provided by monitoring the concentration of  $\text{Cu}^{2+}$  and  $\text{H}^+$  ions during addition of standard base to  $< 10^{-4}$  M  $\text{Cu}(\text{NO}_3)_2$  in 0.10 and 0.010 M  $\text{KNO}_3$  solutions in our earlier research [24,25]. Concentrations of hydrolysed copper species,  $\Sigma \text{Cu}(\text{OH})_n$ , measurable as the difference in  $\text{Cu}^{2+}$  ion concentration levels initially and after each addition of base, was used with the  $\text{H}^+$  ion concentration measurement to evaluate the empirical hydrolysis parameter,  $K_{\text{emp}}^h$ , defined as shown.

$$K_{\text{emp}}^h = \frac{\sum \text{Cu}(\text{OH})_n (\text{H}^+)}{(\text{Cu}^{2+}) K_w} \quad (10)$$

Plots of  $\log K_{\text{emp}}^h$  versus pH at different ionic strengths facilitate the estimation of the quantity of hydrolysed copper species present in the elevated pH region of an experiment.

This computational scheme has been tested by comparing model-based predictions of FA bound copper ion with free  $\text{Cu}^{2+}$  ion based estimates in two kinds of experiments. In the first experiment, base was added to 0.10 M and 0.010 M  $\text{KNO}_3$  solutions containing fulvic acid and copper nitrate at predetermined molar ratios. In the second experiment, copper nitrate solution was added stepwise to 0.10 M and 0.010 M  $\text{KNO}_3$  solutions containing partially neutralized fulvic acid. These experiments and their results are described in detail elsewhere [23]. Agreement of bound copper was, in many instances, quite good. In others there was significant disparity.

In experiments where  $\text{Cu}^{2+}$  was present in excess, model-based predictions of copper ion binding were poorest in the high pH region. Agreement between experiment and model predictions was confined to a restricted pH range. Above a pH of ca. 5.5,  $\text{Cu}^{2+}$  ion binding exceeded stoichiometric based limits and calculated fulvic acid- $\text{Cu}^{2+}$  ion species concentrations using the computational scheme diverged from the experimental values [23].

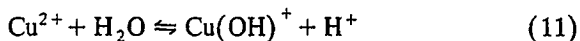
In spite of the instances of failure, this first computational scheme proved quite useful; it accommodated ionic strength disturbances and predicted the  $\text{Cu}^{2+}$  ion binding properties of a soil fulvic acid over a pH range from 3 to 7 while varying metal ion

and fulvic acid concentration levels. The computational scheme permitted calculation of complexed species distributions as a function of the experimental parameters.

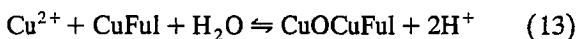
#### *Deficiencies of the computational scheme and recommended refinements*

Disparities between prediction and experiment argue for modification of the computational scheme. Where the quantity of  $\text{Cu}^{2+}$  ion in solution exceeds the metal ion binding capacity of the FA in solution, the computational approach does not predict the almost complete removal of  $\text{Cu}^{2+}$  ion from solution when a pH of ca. 7 is reached. It appears that a FA–Cu ion binding reaction for excess  $\text{Cu}^{2+}$  ion, in the higher pH range has been overlooked in the approach developed.

A candidate reaction path is proposed here (Eqs. 11–13). At a pH > 5.5 hydrolysis of the free  $\text{Cu}^{2+}$  ion that is encountered [24] is insufficient to account for the observed removal of  $\text{Cu}^{2+}$ .



However, the hydrolysis product,  $\text{Cu}(\text{OH})^+$ , can interact with the  $\text{Cu}^{2+}$  ion complexed fulvic acid molecule with release of a proton, forming an oxygen bridged copper fulvic acid complex, as shown, if the copper-complexed products are highly polar. Should this be the case, the net reaction would provide the additional  $\text{Cu}^{2+}$  ion binding path being sought.



Such rationalization is compatible with the protonation properties of the Armadale Horizons Bh fulvic acid during its neutralization with base in the presence of varying quantities of  $\text{Cu}^{2+}$  ion [22]. Design of a step (or steps) to accommodate this complicated phenomenon awaits further study. As a consequence, operations to account for this complexity are not included in the revised computational program.

Such modification of the computational scheme has been found to be unnecessary with copper ion binding to the Suwannee River fulvic acid [24]. With this fulvic acid removal of excess  $\text{Cu}^{2+}$  ion appears to be described adequately by the hydrolysis of the

$\text{Cu}^{2+}$  ion in the 5.5 to 7.5 pH range. Differences in the  $\text{Cu}^{2+}$  ion binding behavior of soil and aquatic fulvic acids illustrated with the approach developed assists in selection of the most suitable computational scheme [22,23].

The main shortcoming of the computational scheme, however, is due to use of information obtained from equating the acid dissociation properties of the  $\text{Cu}^{2+}$  ion containing systems with the  $\text{Cu}^{2+}$  ion free but otherwise equivalent systems. The  $\alpha_0$  obtained from the equilibrium pH of the  $\text{Cu}^{2+}$  ion systems is inaccurate due to modification of carboxylate group ionization patterns and surface charge by  $\text{Cu}^{2+}$  ion complexation. In the computational scheme  $\alpha_0$ , so obtained, is used to evaluate  $(\Delta pK)$ , the Donnan potential term, for estimate of  $\alpha_n$  with Eq. 7. Since the  $\alpha_n$  value is used to calculate the quantity of copper-complexed species formed, an error in the Donnan potential term becomes an increasingly serious source of uncertainty. Defining  $\alpha_0$  obtained from the equilibrium pH of the system as the overall degree of dissociation prior to complexation, an unreasonable assumption becomes the basis of this step of the computational scheme. If  $\alpha_0$  were accurately determined by this procedure, it would still have to be equated with the  $\alpha_n$  values after complexation had taken place, not before.

To remove this deficiency of the computational scheme, use of  $\alpha_0$  has been avoided in the approach that is now proposed. This scheme uses the pH of the  $\text{Cu}^{2+}$  ion containing systems to provide estimates of  $\alpha_0$  only to resolve a first estimate of Donnan potential values. The first step of the computational scheme remains unchanged; the second step using Eq. 7 to evaluate  $\alpha_n$  has been deleted. Instead, Eq. 14 is used to evaluate the quantity of copper complexed by the unidentate weak acid sites (I and III). By taking into account the presence of protonated site I(III) species, use of the  $\alpha_n$  term can be avoided as shown in Eq. 15

$$\begin{aligned} R(\text{COO}_n^-) &= A_n(\text{FA}_i) - \text{CuR}(\text{COO}_n)^+ - \text{HRCOO}_n \\ \beta_{\text{CuR}(\text{COO}_n)^+} &= \frac{\text{CuR}(\text{COO}_n)^+}{(\text{Cu}^{2+})(\Delta pK)^2 \gamma_{\text{CuR}(\text{COO}_n^-)}} \end{aligned} \quad (14)$$

A second equation is provided to permit assessment of the presence of protonated site I(III) species to complete the inventory.

$$\beta_{\text{HR}(\text{COO}_n)} = \frac{\text{HR}(\text{COO}_n)}{(\text{H}^+)(\Delta pK)\gamma_{\text{H}}\text{R}(\text{COO}_n^-)} \quad (15)$$

The equations used to account for  $\text{Cu}^{2+}$  ion binding to sites II and IV are modified similarly. However, in addition to the correction for the presence of the protonated species correction is made for the simultaneous presence of chelated species. The appropriate extra expressions for this formation are also included as shown next.

### 3. The revised computational algorithm

The experimental pH is used to interpolate  $pK_a$  values from a plot of  $pK_a$  versus pH for the ion-free metal, but otherwise equivalent fulvic acid system. These  $pK_a$  values together with the experimental pH value in Eq. 1 give  $\alpha$ . This yields the Donnan potential, the concentration enhancement term for both  $\text{H}^+$  and  $\text{Cu}^{2+}$  ions in the counterion concentrating region of the fulvic acid. Calculation of  $\alpha_n$ , the fractional dissociation of the three carboxylic acid and the one enol site (Eq. 7) is avoided by including the weak acid equilibria as briefly outlined above (Eqs. 14 and 15). Equations used to calculate fulvic acid species are presented in the order of their use in this revised computational approach.

Eqs. 14 and 15 are employed first to estimate the quantities of copper and hydrogen bound to the carboxylate groups associated with Site I and Site III. The material balance based Eq. 16 provides a representation of the quantity of uninvolved Site I and Site III carboxylate to be used in these equations.

$$\begin{aligned} \sum \text{RCOO}_n^- &= A_n(\text{FA}_i) - \sum \text{CuRCOO}_n^+ \\ &\quad - \sum \text{HRCOO}_n \end{aligned} \quad (16)$$

Similar treatment of the speciation estimates for Site II via the salicylic acid and the amino carboxylic acid paths accessible to the copper lead to use of the sets of equations presented below:

#### Salicylic acid path

$$\begin{aligned} K_{\text{Cu}(\text{COO}_{\text{II}})\text{RCO}} &= \frac{\text{Cu}(\text{COO}_{\text{II}})\text{R}(\text{CO})(a_{\text{H}^+})}{(\text{Cu}_i^{2+})(\gamma_{\text{Cu}^{2+}})\text{antilog}(\Delta pK)\left(\sum (\text{COO}^-)\text{R}(\text{COH})\right)} \end{aligned} \quad (17)$$

$$\begin{aligned} \beta_{\text{Cu}(\text{COO}_{\text{II}})\text{R}(\text{COH})^+} &= \frac{\text{Cu}(\text{COO}_{\text{II}})\text{R}(\text{COH})^+}{(\text{Cu}_i^{2+})(\gamma_{\text{Cu}^{2+}})\text{antilog}(\Delta pK)^2\left(\sum (\text{COO}_{\text{II}}^-)\text{R}(\text{COH})\right)} \end{aligned} \quad (18)$$

$$\begin{aligned} \beta_{\text{H}(\text{COO}_{\text{II}})\text{R}(\text{COH})} &= \frac{\text{H}(\text{COO}_{\text{II}})\text{R}(\text{COH})}{(\text{H}^+)(\gamma_{\text{H}^{2+}})\text{antilog}(\Delta pK)\left(\sum (\text{COO}_{\text{II}}^-)\text{R}(\text{COH})\right)} \end{aligned} \quad (19)$$

where

$$\begin{aligned} \sum (\text{COO}^-)\text{R}(\text{OH}) &= ((A_{\text{II}} - 0.07)(\text{FA}_i)) - (\text{Cu}(\text{COO}_{\text{II}})\text{R}(\text{CO})) \\ &\quad - (\text{Cu}(\text{COO}_{\text{II}})\text{R}(\text{COH})^+) \\ &\quad - (\text{HCOO}_{\text{II}}\text{R}(\text{COH})) \end{aligned} \quad (20)$$

#### Aminocarboxylic acid path

$$\begin{aligned} K_{\text{Cu}(\text{COO}_{\text{II}})\text{R}(\text{NH}_2)^+} &= \frac{\text{Cu}(\text{COO}_{\text{II}})\text{R}(\text{NH}_2)^+(a_{\text{H}^+})}{(\text{Cu}_i^{2+})(\gamma_{\text{Cu}^{2+}})\text{antilog}(\Delta pK)\left(\sum (\text{COO}_{\text{II}}^-)\text{R}(\text{NH}_3)\right)} \end{aligned} \quad (21)$$

$$\begin{aligned} \beta_{\text{Cu}(\text{COO}_{\text{II}})\text{R}(\text{NH}_3)^{2+}} &= \frac{\text{Cu}(\text{COO}_{\text{II}})\text{R}(\text{NH}_3)^{2+}}{(\text{Cu}_i^{2+})(\gamma_{\text{Cu}^{2+}})\text{antilog}(\Delta pK)^2\left(\sum (\text{COO}_{\text{II}}^-)\text{R}(\text{NH}_3)\right)} \end{aligned} \quad (22)$$

$$\begin{aligned} \beta_{\text{H}(\text{COO}_{\text{II}})\text{R}(\text{NH}_3)^+} &= \frac{\text{H}(\text{COO}_{\text{II}})\text{R}(\text{NH}_3)^+}{(\text{H}^+)(\gamma_{\text{H}^+})\text{antilog}(\Delta pK)\left(\sum (\text{COO}_{\text{II}}^-)\text{R}(\text{NH}_3)\right)} \end{aligned} \quad (23)$$

where

$$\begin{aligned} & \sum (\text{COO}_{\text{II}}^-) \text{R}(\text{NH}_3) \\ &= (\text{A}_{\text{II}} - 0.23)(\text{FA}_i) - \text{Cu}(\text{COO}_{\text{II}}) \text{R}(\text{NH}_2)^+ \\ & \quad - \text{Cu}(\text{COO}_{\text{II}}) \text{R}(\text{NH}_3)^{2+} \\ & \quad - \text{H}(\text{COO}_{\text{II}}) \text{R}(\text{NH}_3) \end{aligned} \quad (24)$$

Finally the complexation possibilities (uni- and bidentate) accessible to the *enol* groups constituting site IV are treated in a manner paralleling the approach used to anticipate the binding of  $\text{Cu}^{2+}$  ion via both the salicylic acid and the aminocarboxylic acid paths presumed operable in the Site II bidentate complex formation processes.

#### Dihydroxyl path

$$\begin{aligned} & K_{\text{Cu}(\text{COO}_{\text{IV}})\text{CRCO}} \\ &= \frac{\text{Cu}(\text{COO}_{\text{IV}})\text{CRCO}(a_{\text{H}^+})}{(\text{Cu}_f^{2+})(\gamma_{\text{Cu}^{2+}})\text{antilog}(\Delta pK) \left( \sum (\text{COO}_{\text{IV}}^-)\text{CRCOH} \right)} \end{aligned} \quad (25)$$

$$\begin{aligned} & \beta_{\text{Cu}(\text{COO}_{\text{IV}})\text{CRCOH}^+} \\ &= \frac{\text{Cu}(\text{COO}_{\text{IV}})\text{CRCOH}^+}{(\text{Cu}_f^{2+})(\gamma_{\text{Cu}^{2+}})\text{antilog}(\Delta pK)^2 \left( \sum (\text{COO}_{\text{IV}}^-)\text{CRCOH} \right)} \end{aligned} \quad (26)$$

$$\begin{aligned} & \beta_{\text{H}(\text{COO}_{\text{IV}})\text{CRCOH}} \\ &= \frac{\text{H}(\text{COO}_{\text{IV}})\text{CRCOH}}{(\text{H}^+)(\gamma_{\text{H}^+})\text{antilog}(\Delta pK) \left( \sum (\text{COO}_{\text{IV}}^-)\text{CRCOH} \right)} \end{aligned} \quad (27)$$

where

$$\begin{aligned} & \sum \text{CO}_{\text{IV}} \text{CRCOH} \\ &= \text{A}_{\text{IV}}(0.9)(\text{FA}_i) - \text{Cu}(\text{CO}_{\text{IV}})\text{CRCO} \\ & \quad - \text{Cu}(\text{CO}_{\text{IV}})\text{CRCOH}^+ - \text{H}(\text{CO}_{\text{IV}}\text{CRCOH}) \end{aligned} \quad (28)$$

#### keto-enol path

$$\begin{aligned} & \beta_{\text{Cu}(\text{COO}_{\text{IV}})\text{CRCO}^+} \\ &= \frac{\text{Cu}(\text{COO}_{\text{IV}})\text{CRCO}^+}{(\text{Cu}_f^{2+})(\gamma_{\text{Cu}^{2+}})\text{antilog}(\Delta pK)^2 \left( \sum (\text{COO}_{\text{IV}}^-)\text{CRCO} \right)} \end{aligned} \quad (29)$$

where

$$\beta_{\text{H}(\text{COO}_{\text{IV}})\text{CRCO}^+} = \frac{\text{H}(\text{COO}_{\text{IV}})\text{CRCO}^+}{(\text{H}^+)(\gamma_{\text{H}^+})\text{antilog}(\Delta pK) \left( \sum (\text{COO}_{\text{IV}}^-)\text{CRCO} \right)} \quad (30)$$

$$\begin{aligned} & \sum \text{CO}_{\text{IV}}^- \text{CRCO} \\ &= \text{A}_{\text{IV}}(0.1)(\text{FA}_i) - \text{Cu}(\text{CO}_{\text{IV}})\text{CRCO}^+ \\ & \quad - \text{H}(\text{CO}_{\text{IV}}\text{CRCO}) \end{aligned} \quad (31)$$

To account for removal of  $\text{Cu}^{2+}$  ion by hydrolysis Eq. 10 is used as it was in the original computational scheme when the pH exceeds 5.5. Solution of Eq. 10 and each set of simultaneous equations provided by this approach produces the first series of copper binding estimates once a pCu value is selected to initiate the sequence of computations at a particular experimental pH. Their sum is added to the free copper ion (pCu) for comparison with the total quantity of copper in the system under investigation. If there is a discrepancy between the two numbers another pCu value is selected and the series of computations are repeated. Such iteration, performed manually using the Smart Spreadsheet with Graphics program, is continued until the selected pCu value affects the material balance being sought.

This initial assessment of  $\text{Cu}^{2+}$  ion binding to the Armadale fulvic acid bases estimate of the Donnan potential term on the acid dissociation properties of the fulvic acid in the absence of  $\text{Cu}^{2+}$ . With the unidentate  $\text{CuA}^+$  species concentrations calculated in the first iteration of the computational scheme correction for screening of the negative fulvate ion charge by  $\sum \text{CuA}^+$  can be made to permit a more accurate estimate of the Donnan potential term than before for use in a second iteration of the program. The  $(\Delta pK)$  versus  $\alpha$  plots [22] employ  $\alpha_{\text{eff}}$ , defined as shown, for this purpose

$$\begin{aligned} & \alpha_{\text{eff}} = \frac{\sum A_{\text{eff}}}{\text{FA}_i} \\ & \sum A_{\text{eff}} = bV_b + hV_s - \sum \text{CuA}^+ - \sum \text{CuAA}' \end{aligned} \quad (32)$$

In the above equation,  $\alpha_{\text{eff}}$  is the effective degree of FA dissociation,  $\sum \text{CuA}^+$  is the fraction of fulvic

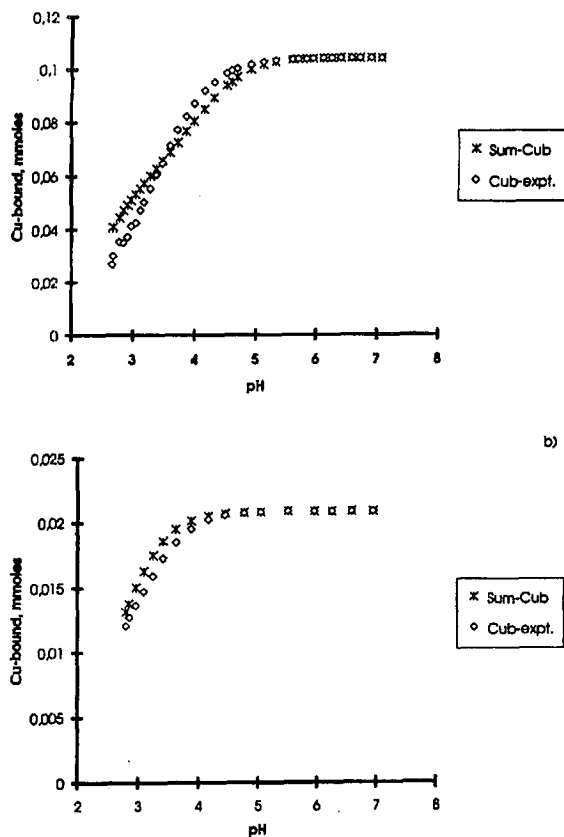


Fig. 1. Comparison of experimental-based (Cub-expt) and model-based estimates of bound copper (Sum-Cub) during neutralization of a 0.10 M  $\text{KNO}_3$  solution: (a) contain 0.4989 mmol of Armadale Horizons Bh fulvic acid in the presence of 0.1044 millimoles of copper nitrate; (b) 0.2883 mmol of Armadale Horizon Bh fulvic acid in the presence of 0.02088 mmol of copper nitrate.

acid sites which exist as singly positively charged Cu site complexes, with  $b$  and  $h$  corresponding respectively to the concentration of standard base added and the solution concentration of  $\text{H}^+$  ion after each addition of base,  $V_b$  representing the volume of base added and  $V_s$  the volume of the solution after each addition, and  $\Sigma\text{CuAA}'$  accounting for the total of Cu chelated species formed.

The computation continues until [22] the sum of all calculated  $\text{Cu}^{2+}$  ion containing species ( $\Sigma\text{Cu}^{2+} + \Sigma\text{CuA}^+ + \Sigma\text{CuAA}'$ ) equals  $\Sigma\text{Cu}_{\text{total}}$ , the quantity of  $\text{Cu}^{2+}$  ions added to the system and [23] the  $\Sigma\text{CuA}^+$  value agrees with the  $\Sigma\text{CuA}^+$  value selected to resolve the Donnan potential term.

Readjustment in two operations of the first computational scheme was introduced in the revised approach. The accuracy of the operation which involved use of the Donnan potential versus  $\alpha_o$  plots to evaluate  $\alpha_n$  was enhanced by a more precise analysis, than before, of the acid dissociation data they were based upon [23]. In the operation used to account for the chelation of copper by the dihydroxyl group (site IV) the equilibrium constant of  $2 \times 10^{-2}$  used earlier [23] in the mass action expression for the displacement reaction (Eq. 9) employed for this purpose (Eq. 27 in the revised program) was increased by a factor of 10. By raising the second dissociation constant,  $K_a$ , of the dihydroxyl from  $2 \times 10^{-2}$  to

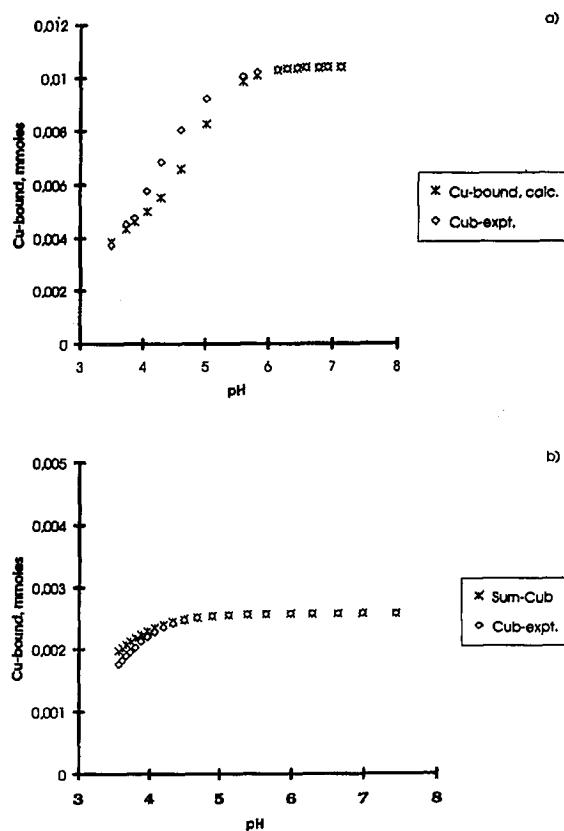


Fig. 2. Comparison of experimental-based (Cub-expt) and model-based estimates of bound copper (Cu-bound,calc) during neutralization of a 0.010 M  $\text{KNO}_3$  solution: (a) 0.04399 mmol of Armadale Horizons Bh fulvic acid in the presence of 0.01044 mmol of copper nitrate; (b) 0.04075 mmol of Armadale Horizons Bh fulvic acid in the presence of 0.002575 mmol of copper nitrate.

$2 \times 10^{-1}$  for this purpose correlation of experiment with computation was improved to justify this modification of the first computational scheme.

#### 4. Results from the application of the algorithm

Calculated species distribution using this algorithm for four representative fulvic acid, copper nitrate, potassium nitrate systems are presented in Table 1. These results are also summarized in Figs. 1 and 2. In these figures the experimental and model-based estimates of bound copper for each of the systems are plotted versus  $p\{H\}$ . The complete  $p\{H\}$  range examined in these studies has been included in these figures. Even when the molar ratio of FA to  $\text{Cu}^{2+}$  is varied sizeably while the salt concentration level is varied by a factor of ten there is no noticeable effect on prediction of copper ion binding to the fulvic acid over a pH range of ca. 3–7. Copper complexed species formed with the various fulvic acid sites in the course of fulvic acid neutralization with standard base is presented in Fig. 3 to provide an example of the speciation tendencies of the FA,  $\text{Cu}(\text{NO}_3)_2$ ,  $\text{KNO}_3$  systems examined in Table 1. From this kind of projection insights with respect to the part that each complexation site plays as a function of  $p\{H\}$  and the copper to fulvic acid ratio in the solution are

gained. The dominant role of the bidentate ligands when the quantity of copper is much smaller than the fulvic acid capacity for it becomes obvious.

Results obtained with the algorithm for the additional systems examined earlier with the first computational scheme in Ref. [23] (except for those in which the quantity of  $\text{Cu}^{2+}$  exceeded the capacity of the fulvic acid) are available upon request.

Overall, the algorithm-based predictions of free and bound copper compare favorably with the experimentally-based values of these parameters. Development of this algorithm for the prediction of metal ion binding by organic acids in natural waters, once characterized as described, has been demonstrated. This approach has promising compatibility with chemical speciation programs that are already available for the consideration of ion binding by inorganic ligands in natural waters.

#### 5. Conclusions

A scheme which provides the capability of describing metal ion binding by a fulvic acid once the  $p\{H\}$  of the system is known has been developed. A thorough estimation of the acidic moieties constituting the fulvic acid molecule is a requisite for such scheme to be successful. In our approach, the fulvic

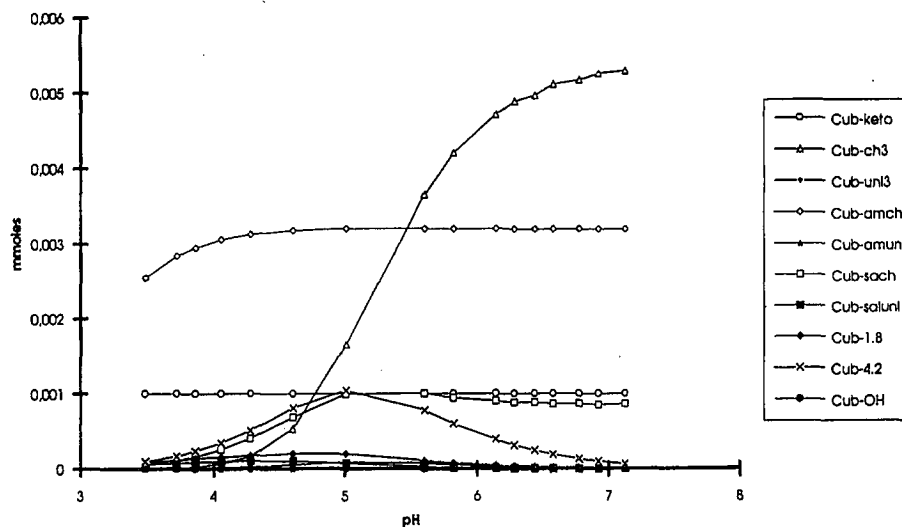


Fig. 3. The copper fulvate species distribution plot in a 0.010 M  $\text{KNO}_3$  solution containing 0.04399 mmol of Armadale Horizons Bh fulvic acid and 0.01044 mmol of copper nitrate in the course of its neutralization with standard base.

Table 1  
The p(H)-based prediction of copper ion binding to fulvic acid

(a) System: 0.4989 mmol Armadale Horizons Bh fulvic acid, initial					
ml/base	p(H)	pCu <sub>(exp)</sub>	pCu <sub>(calc)</sub>	$\Sigma\text{Cu}_{b,(\text{exp})}$	$\Sigma\text{Cu}_{b,(\text{calc})}$
0.00	2.672	2.818	2.910	$2.685 \times 10^{-2}$	$4.161 \times 10^{-2}$
0.10	2.684	2.837	2.920	$3.003 \times 10^{-2}$	$4.185 \times 10^{-2}$
0.50	2.780	2.873	2.940	$3.541 \times 10^{-2}$	$4.601 \times 10^{-2}$
0.80	2.853	2.873	2.973	$3.500 \times 10^{-2}$	$4.833 \times 10^{-2}$
1.00	2.914	2.889	2.989	$3.726 \times 10^{-2}$	$5.062 \times 10^{-2}$
1.20	2.973	2.918	3.010	$4.135 \times 10^{-2}$	$5.254 \times 10^{-2}$
1.40	3.045	2.928	3.028	$4.255 \times 10^{-2}$	$5.508 \times 10^{-2}$
1.60	3.119	2.964	3.050	$4.725 \times 10^{-2}$	$5.717 \times 10^{-2}$
1.80	3.184	2.990	3.070	$5.037 \times 10^{-2}$	$5.951 \times 10^{-2}$
2.00	3.286	3.035	3.110	$5.550 \times 10^{-2}$	$6.231 \times 10^{-2}$
2.20	3.382	3.084	3.140	$6.056 \times 10^{-2}$	$6.533 \times 10^{-2}$
2.40	3.485	3.129	3.180	$6.472 \times 10^{-2}$	$6.833 \times 10^{-2}$
2.60	3.599	3.210	3.220	$7.135 \times 10^{-2}$	$7.210 \times 10^{-2}$
2.80	3.723	3.297	3.270	$7.725 \times 10^{-2}$	$7.618 \times 10^{-2}$
3.00	3.859	3.388	3.340	$8.230 \times 10^{-2}$	$8.006 \times 10^{-2}$
3.20	3.995	3.498	3.425	$8.718 \times 10^{-2}$	$8.320 \times 10^{-2}$
3.40	4.156	3.637	3.525	$9.185 \times 10^{-2}$	$8.736 \times 10^{-2}$
3.60	4.309	3.770	3.630	$9.513 \times 10^{-2}$	$9.100 \times 10^{-2}$
3.80	4.518	3.964	3.794	$9.845 \times 10^{-2}$	$9.504 \times 10^{-2}$
3.90	4.597	4.052	3.860	$9.953 \times 10^{-2}$	$9.605 \times 10^{-2}$
4.00	4.691	4.133	3.950	$1.040 \times 10^{-1}$	$9.736 \times 10^{-2}$
4.20	4.919	4.353	4.170	$1.020 \times 10^{-1}$	$1.003 \times 10^{-1}$
4.40	5.128	4.541	4.390	$1.028 \times 10^{-1}$	$1.024 \times 10^{-1}$
4.60	5.326	4.745	4.625	$1.034 \times 10^{-1}$	$1.025 \times 10^{-1}$
4.80	5.616	4.987	4.970	$1.038 \times 10^{-1}$	$1.030 \times 10^{-1}$
4.90	5.702	5.091	5.070	$1.039 \times 10^{-1}$	$1.033 \times 10^{-1}$
5.00	5.841	5.188	5.220	$1.040 \times 10^{-1}$	$1.048 \times 10^{-1}$
5.10	5.947	5.305	5.355	$1.041 \times 10^{-1}$	$1.037 \times 10^{-1}$
5.20	6.119	5.415	5.550	$1.042 \times 10^{-1}$	$1.038 \times 10^{-1}$
5.30	6.255	5.577	5.690	$1.043 \times 10^{-1}$	$1.049 \times 10^{-1}$
5.40	6.403	5.651	5.860	$1.043 \times 10^{-1}$	$1.041 \times 10^{-1}$
5.50	6.583	5.810	6.050	$1.043 \times 10^{-1}$	$1.043 \times 10^{-1}$
5.60	6.724	5.965	6.200	$1.043 \times 10^{-1}$	$1.040 \times 10^{-1}$
5.70	6.910	6.092	6.390	$1.044 \times 10^{-1}$	$1.043 \times 10^{-1}$
5.80	7.078	6.279	6.570	$1.044 \times 10^{-1}$	$1.036 \times 10^{-1}$
(b) System: 0.2883 mmol Armadale Horizons Bh fulvic acid, initial					
ml/base	p(H)	pCu <sub>(exp)</sub>	pCu <sub>(calc)</sub>	$\Sigma\text{Cu}_{b,(\text{exp})}$	$\Sigma\text{Cu}_{b,(\text{calc})}$
0.00	2.799	3.659	3.720	$1.206 \times 10^{-2}$	$1.321 \times 10^{-2}$
0.20	2.856	3.694	3.760	$1.271 \times 10^{-2}$	$1.384 \times 10^{-2}$
0.40	2.970	3.749	3.845	$1.364 \times 10^{-2}$	$1.510 \times 10^{-2}$
0.60	3.096	3.821	3.955	$1.472 \times 10^{-2}$	$1.629 \times 10^{-2}$
0.80	3.243	3.917	4.090	$1.592 \times 10^{-2}$	$1.754 \times 10^{-2}$
1.00	3.410	4.058	4.255	$1.728 \times 10^{-2}$	$1.863 \times 10^{-2}$
1.20	3.620	4.237	4.480	$1.848 \times 10^{-2}$	$1.950 \times 10^{-2}$
1.40	3.878	4.492	4.760	$1.954 \times 10^{-2}$	$2.012 \times 10^{-2}$
1.60	4.162	4.818	5.063	$2.024 \times 10^{-2}$	$2.050 \times 10^{-2}$
1.80	4.442	5.149	5.355	$2.058 \times 10^{-2}$	$2.070 \times 10^{-2}$
2.00	4.762	5.499	5.685	$2.075 \times 10^{-2}$	$2.082 \times 10^{-2}$
2.20	5.044	5.819	5.980	$2.082 \times 10^{-2}$	$2.082 \times 10^{-2}$
2.40	5.526	6.304	6.480	$2.086 \times 10^{-2}$	$2.090 \times 10^{-2}$
2.60	5.957	6.744	6.938	$2.087 \times 10^{-2}$	$2.082 \times 10^{-2}$

Table 1 (continued)

(b) System: 0.2883 mmol Armadale Horizons Bh fulvic acid, initial					
ml/base	p{H}	pCu <sub>(exp)</sub>	pCu <sub>(calc)</sub>	$\Sigma\text{Cu}_{b,(exp)}$	$\Sigma\text{Cu}_{b,(calc)}$
2.70	6.254	7.047	7.242	$2.088 \times 10^{-2}$	$2.088 \times 10^{-2}$
2.80	6.584	7.401	7.580	$2.088 \times 10^{-2}$	$2.087 \times 10^{-2}$
2.90	6.945	7.728	7.945	$2.088 \times 10^{-2}$	$2.087 \times 10^{-2}$
(c) System: 0.04399 mmol Armadale Horizons Bh fulvic acid, initial					
ml/base	p{H}	pCu <sub>(exp)</sub>	pCu <sub>(calc)</sub>	$\Sigma\text{Cu}_{b,(exp)}$	$\Sigma\text{Cu}_{b,(calc)}$
0.00	3.496	3.874	3.900	$3.744 \times 10^{-3}$	$4.118 \times 10^{-3}$
1.00	3.726	3.936	3.955	$4.519 \times 10^{-3}$	$4.736 \times 10^{-3}$
1.50	3.863	3.958	3.990	$4.756 \times 10^{-3}$	$5.111 \times 10^{-3}$
2.00	4.057	4.048	4.040	$5.775 \times 10^{-3}$	$5.706 \times 10^{-3}$
2.50	4.282	4.166	4.120	$6.851 \times 10^{-3}$	$6.444 \times 10^{-3}$
3.00	4.605	4.345	4.275	$8.041 \times 10^{-3}$	$7.554 \times 10^{-3}$
3.50	5.009	4.645	4.535	$9.226 \times 10^{-3}$	$8.872 \times 10^{-3}$
4.00	5.597	5.145	5.050	$1.005 \times 10^{-2}$	$1.003 \times 10^{-2}$
4.20	5.818	5.390	5.275	$1.022 \times 10^{-2}$	$1.019 \times 10^{-2}$
4.40	6.144	5.675	5.600	$1.032 \times 10^{-2}$	$1.030 \times 10^{-2}$
4.50	6.287	5.832	5.750	$1.036 \times 10^{-2}$	$1.031 \times 10^{-2}$
4.60	6.440	5.938	5.890	$1.038 \times 10^{-2}$	$1.038 \times 10^{-2}$
4.70	6.580	6.117	6.040	$1.040 \times 10^{-2}$	$1.043 \times 10^{-2}$
4.80	6.777	6.285	6.235	$1.041 \times 10^{-2}$	$1.039 \times 10^{-2}$
4.90	6.921	6.460	6.385	$1.042 \times 10^{-2}$	$1.046 \times 10^{-2}$
5.00	7.127	6.635	6.590	$1.043 \times 10^{-2}$	$1.037 \times 10^{-2}$
(d) System: 0.04075 mmol Armadale Horizons Bh fulvic acid, initial					
ml/base	p{H}	pCu <sub>(exp)</sub>	pCu <sub>(calc)</sub>	$\Sigma\text{Cu}_{b,(exp)}$	$\Sigma\text{Cu}_{b,(calc)}$
0.00	3.562	4.790	4.930	$1.760 \times 10^{-3}$	$1.997 \times 10^{-3}$
0.20	3.613	4.828	4.982	$1.825 \times 10^{-3}$	$2.027 \times 10^{-3}$
0.40	3.666	4.870	5.018	$1.892 \times 10^{-3}$	$2.089 \times 10^{-3}$
0.60	3.724	4.915	5.075	$1.957 \times 10^{-3}$	$2.123 \times 10^{-3}$
0.80	3.796	4.974	5.128	$2.033 \times 10^{-3}$	$2.196 \times 10^{-3}$
1.00	3.873	5.057	5.200	$2.126 \times 10^{-3}$	$2.242 \times 10^{-3}$
1.20	3.964	5.144	5.275	$2.206 \times 10^{-3}$	$2.311 \times 10^{-3}$
1.40	4.065	5.248	5.370	$2.283 \times 10^{-3}$	$2.359 \times 10^{-3}$
1.60	4.187	5.380	5.490	$2.359 \times 10^{-3}$	$2.399 \times 10^{-3}$
1.80	4.328	5.536	5.625	$2.423 \times 10^{-3}$	$2.443 \times 10^{-3}$
2.00	4.490	5.703	5.775	$2.471 \times 10^{-3}$	$2.495 \times 10^{-3}$
2.20	4.678	5.926	5.965	$2.512 \times 10^{-3}$	$2.513 \times 10^{-3}$
2.40	4.891	6.171	6.175	$2.539 \times 10^{-3}$	$2.536 \times 10^{-3}$
2.60	5.125	6.459	6.408	$2.557 \times 10^{-3}$	$2.550 \times 10^{-3}$
2.80	5.385	6.771	6.670	$2.566 \times 10^{-3}$	$2.556 \times 10^{-3}$
3.00	5.652	7.101	6.943	$2.571 \times 10^{-3}$	$2.554 \times 10^{-3}$
3.20	5.985	7.465	7.268	$2.573 \times 10^{-3}$	$2.584 \times 10^{-3}$
3.40	6.283	7.802	7.577	$2.574 \times 10^{-3}$	$2.572 \times 10^{-3}$
3.60	6.645	8.121	7.940	$2.525 \times 10^{-3}$	$2.577 \times 10^{-3}$
3.80	6.983	8.492	8.283	$2.575 \times 10^{-3}$	$2.572 \times 10^{-3}$
4.00	7.439	8.919	8.740	$2.575 \times 10^{-3}$	$2.569 \times 10^{-3}$

acid has been conceptualised as an assemblage of amphiphilic acidic moieties with 4 to 5 predominant sites whose average acidic strengths vary. This scheme has been demonstrated with the  $\text{Cu}^{2+}$ , soil

fulvic acid, and  $\text{NaNO}_3$  ( $\text{KNO}_3$ ) system. The algorithm that has been developed for this purpose relies strongly on the formation constants reported for the interaction between  $\text{Cu}^{2+}$  ions and the envisaged

functionalities of the acidic sites of the fulvic acid and is suitable for incorporation into already existent chemical speciations programs [15].

## References

- [1] R.L. Wershaw, *J. Contam. Hydrol.*, 1 (1986) 29.
- [2] G. Sposito, K.M. Holtzclaw and D.A. Keech (1977), *J. Am. Soil Sci. Soc.*, 41 (1977) 1119.
- [3] B.M. Bartschat, S.E. Cabaniss and F.M.M. Morel, *Environ. Sci. Technol.*, 26 (1992) 284.
- [4] J.H. Ephraim, M.M. Reddy and J.A. Marinsky, *Humic Substances in the Aquatic and Terrestrial Environment*, Lecture Notes in Earth Science, 33 (1991) 263.
- [5] E. Tipping and M.A. Hurley, *Geochim. Cosmochim. Acta*, 56 (1992) 3627.
- [6] M.S. Shuman, B.J. Collins, P.J. Fitzgerald and D.L. Olson, in R.F. Christmann and E.T. Gjessing (Eds.), *Aquatic and Terrestrial Humic Materials*, Ann Arbor Science Press, Ann Arbor, MI, 1983, pp. 349–370.
- [7] J. Buffle and R.S. Altman, in W. Stumm (Ed.), *Aquatic Surface Chemistry*, Wiley, New York, 1987, Chap. 13.
- [8] J.C.M. de Wit, W.H. van Riemsdijk, M.M. Nederlof, D.G. Kiniburg and L.K. Koopal, *Anal. Chim. Acta*, 232 (1990) 189.
- [9] E.M. Perdue and C.R. Lytle, *Environ. Sci. Technol.*, 17 (1983) 654.
- [10] E.M. Perdue and R.S. Parrish, *Comput. Geosci.*, 13 (1987) 587.
- [11] R.S. Altmann and J. Buffle, *Geochim. Cosmochim. Acta*, 52 (1988) 1505.
- [12] D.S. Gamble and C.H. Langford, *Environ. Sci. Technol.*, 22 (1988) 1325.
- [13] D.S. Gamble, A.W. Underdown and C.H. Langford, *Anal. Chem.*, 52 (1980) 1901.
- [14] A. Fitch and F.J. Stevenson, *J. Am. Soil Sci. Soc.*, 48 (1984) 1044.
- [15] J.C. Westall, J.L. Zachary and F.M.M. Morel, *MINEQL*, A Computer Program for the Calculation of the Chemical Equilibrium Composition of Aqueous Systems, Tech Note 18, Civil Eng., Massachusetts Institute of Technology, Cambridge, MA, 1976.
- [16] D.A. Dzombak, W. Fish and F.M.M. Morel, *Environ. Sci. Technol.*, 20 (1986) 669.
- [17] E. Tipping, *Environ. Sci. Technol.*, 27 (1993) 520.
- [18] J.A. Marinsky, S. Gupta and R. Schindler, *J. Colloids Interface Sci.*, 89 (1982) 401.
- [19] J.A. Marinsky, M.M. Reddy, J. Ephraim and A. Mathuthu, *Ion Binding by Humic and Fulvic Acids: A Computational Procedure Based on Functional Site Heterogeneity and the Physical Chemistry of Polyelectrolyte Solutions*, SKB Technical Report 88-01 (1988).
- [20] J.A. Marinsky, *Ion Exchange and Solvent Extraction*, 11 (1993) 237.
- [21] J.A. Marinsky and J. Ephraim, *Environ. Sci. Technol.*, 20 (1986) 349.
- [22] J.H. Ephraim, A.S. Mathuthu, S. Alegret, M. Bicking, R.L. Malcolm and J.A. Marinsky, *Environ. Sci. Technol.*, 20 (1986) 354.
- [23] J.H. Ephraim and J.A. Marinsky, *Environ. Sci. Technol.*, 20 (1986) 367.
- [24] J.H. Ephraim, Ph.D. Thesis, State University of New York at Buffalo, NY, 1985.
- [25] A.S. Mathuthu, Ph.D. Thesis, State University of New York at Buffalo, NY, 1987.
- [26] J.H. Ephraim, J.A. Marinsky and S.J. Cramer, *Talanta*, 36 (1989) 437.
- [27] L.G. Sillén and A. Martell, Supplement No. 1, *Stability Constants of Metal Ion Complexes*, The Chemical Society, London, 1971.
- [28] M. Lloyd, V. Wycherley and C.B. Monk, *J. Chem. Soc.*, 1951, 1786.
- [29] J. Kielland, *J. Am. Chem. Soc.*, 59 (1937) 1675.